

Polymorphism in High-Crystalline-Stability Metal–Organic Nanotubes

Fangna Dai, Haiyan He, and Daofeng Sun*

Key Lab of Colloid and Interface Chemistry, Ministry of Education, School of Chemistry and Chemical Engineering, Shandong University, Jinan 250100, People's Republic of China

Received February 12, 2009

By application of mixed organic ligands of 5-amino-2,4,6-triiodoisophthalic acid (H₂ATIBDC) and 4,4'-bipyridine (bpy) to assemble with Zn ions at room temperature, two novel polymorphic structures, Zn(ATIBDC)(bpy)·3H₂O (denoted as **MONT-1** and **MONT-2**), possessing one-dimensional metal–organic nanotubular structures have been synthesized and characterized. **MONT-1** was generated by connection of the zero-dimensional Zn-bpy squares through the bridging ATIBDC ligands, while **MONT-2** was formed by connection of the one-dimensional Zn-bpy helix through the ATIBDC ligands. Both nanotubes possess highly crystalline stabilities and can absorb the uncoordinated water molecules reversibly.

The existence of polymorphism and interpenetration in supramolecular chemistry and crystal engineering has introduced more elements of complexity in the construction of metal–organic frameworks (MOFs) and coordination networks with desired topological structures and illuminated the difficulty in accurately predicting final structures.^{1–3} As defined by McCrone, polymorphism is “a solid crystalline phase of a given compound with the same molecular formula existing

in at least two different arrangements in the solid state”.⁴ In the past decades, polymorphism in organic crystals and coordination networks has been widely studied and documented.^{5,6} However, polymorphism in noninterpenetrating metal–organic nanotubes is quite rare. To the best of our knowledge, only one example of a nanotubular uranyl phenylphosphonate, (UO₂)₃(HO₃PC₆H₅)₂(O₃PC₆H₅)₂·H₂O, has been reported so far.⁷

On the other hand, the study of polymorphic structures may gain a better understanding of the factors that influence the crystal growth and lead to the generation of novel MOFs.^{1a} It has been documented that, for an angular node generated by a cis-substituted metal moiety and a linear linker, there are at least three possible isomers: a zero-dimensional (0D) square, a one-dimensional (1D) zigzag chain, and a 1D helix (Scheme 1). The discrete “square box” or “molecular square” based on linear linkers has been designed and characterized by the groups of Stang,⁸ Hupp,⁹ and Fujita.¹⁰ The 1D zigzag chain has also been widely explored in the past decades.¹¹ Compared to the 0D square and 1D zigzag chain, reports on the 1D helix are somewhat rare.¹²

From a design perspective, the simple isomer may act as subunits, which can be linked by a secondary organic ligand to generate novel isomeric MOFs such as metal–organic nanotubes with desired topologies. Compared to the

*To whom correspondence should be addressed. E-mail: dfsun@sdu.edu.cn.

(1) (a) Moulton, B.; Zaworotko, M. J. *Chem. Rev.* **2001**, *101*, 1629–1658. (b) Tabellion, F. M.; Seidel, S. R.; Arif, A. M.; Stang, P. J. *J. Am. Chem. Soc.* **2001**, *123*, 7740–7741. (c) Hennigar, T. L.; MacQuarrie, D. C.; Losier, P.; Rogers, R. D.; Zaworotko, M. J. *Angew. Chem., Int. Ed. Engl.* **1997**, *36*, 972–973. (d) Swift, J. A.; Pivovar, A. M.; Reynolds, A. M.; Ward, M. D. *J. Am. Chem. Soc.* **1998**, *120*, 5887–5894.

(2) (a) Masaoka, S.; Tanaka, D.; Nakanishi, Y.; Kitagawa, S. *Angew. Chem., Int. Ed.* **2004**, *43*, 2530–2534. (b) Batten, S. R.; Robson, R. *Angew. Chem., Int. Ed.* **1998**, *37*, 1460–1494 and references cited therein.

(3) (a) Reineke, T. M.; Eddaoudi, M.; Moler, D.; O’Keeffe, M.; Yaghi, O. M. *J. Am. Chem. Soc.* **2000**, *122*, 4843–4844. (b) Kesanli, B.; Cui, Y.; Smith, M. R.; Bittner, E. W.; Bockrath, B. C.; Li, W. B. *Angew. Chem., Int. Ed.* **2005**, *44*, 72–75.

(4) (a) McCrone, W. C. In *Physics and Chemistry of the Organic Solid State*; Fox, D., Labes, M. M., Eds.; Wiley-Interscience: New York, 1965; Vol. 2, pp 725–767.

(5) (a) Kobayashi, K.; Sato, A.; Sakamoto, S.; Yamaguchi, K. *J. Am. Chem. Soc.* **2003**, *125*, 3035–3045. (b) Cicero, R. L.; Zhao, D.; Protasiewicz, J. D. *Inorg. Chem.* **1996**, *35*, 275–276. (c) Soldatov, D. V.; Enright, G. D.; Ripmeester, J. A. *Cryst. Growth Des.* **2004**, *4*, 1185–1194. (d) Mandal, S.; Natarajan, S. *Inorg. Chem.* **2008**, *47*, 5304–5313.

(6) (a) Liu, X. G.; Bao, S. S.; Li, Y. Z.; Zheng, L. M. *Inorg. Chem.* **2008**, *47*, 5525–5527. (b) Rao, V. K.; Chakrabarti, S.; Natarajan, S. *Inorg. Chem.* **2007**, *46*, 10781–10790. (c) Chen, X. D.; Wu, H. F.; Zhao, X. H.; Zhao, X. J.; Du, M. *Cryst. Growth Des.* **2007**, *7*, 124–131.

(7) Aranda, M. A. G.; Cabeza, A.; Bruque, S.; Poojary, D. M.; Clearfield, A. *Inorg. Chem.* **1998**, *37*, 1827–1832.

(8) For reviews, see: (a) Stang, P. J.; Olenyuk, B. *Acc. Chem. Res.* **1997**, *30*, 502–518. (b) Leininger, S.; Olenyuk, B.; Stang, P. J. *Chem. Rev.* **2000**, *100*, 853–907.

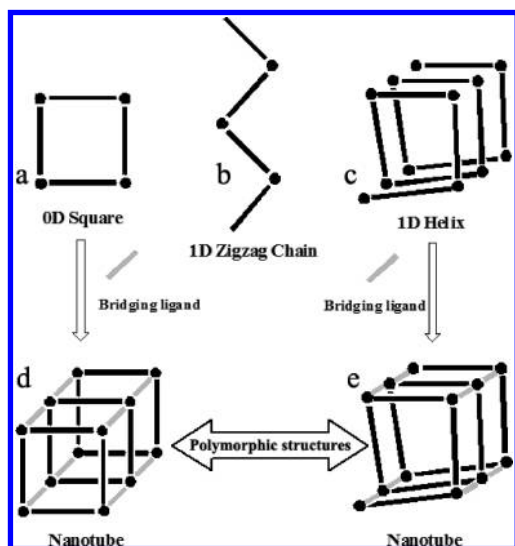
(9) (a) Slone, R. V.; Yoon, D. I.; Calhoun, R. M.; Hupp, J. T. *J. Am. Chem. Soc.* **1995**, *117*, 11813–11814. (b) Slone, R. V.; Hupp, J. T. *Inorg. Chem.* **1997**, *36*, 5422–5423. (c) Slone, R. V.; Benkstein, K. D.; Belanger, S.; Hupp, J. T.; Guzei, I. A.; Rheingold, A. L. *Coord. Chem. Rev.* **1998**, *171*, 221–243.

(10) Fujita, M.; Sasaki, O.; Mitsuhashi, T.; Fujita, T.; Yazaki, J.; Yamaguchi, K.; Ogura, K. *Chem. Commun.* **1996**, 1535–1536.

(11) (a) Dong, Y. B.; Smith, M. D.; Zur Loye, H. C. *Inorg. Chem.* **2000**, *39*, 1943–1949. (b) Abrahams, B. F.; Lu, K. D.; Moubaraki, B.; Murray, K. S.; Robson, R. *Dalton Trans.* **2000**, 1793–1797. (c) Guo, G. C.; Wang, Q. M.; Mak, T. C. W. *Inorg. Chem. Commun.* **2000**, *3*, 313–315. (d) Stocker, F. B.; Troester, M. A.; Britton, D. *Inorg. Chem.* **1996**, *35*, 3145–3153.

(12) (a) Biradha, K.; Seward, C.; Zaworotko, M. J. *Angew. Chem., Int. Ed.* **1999**, *38*, 492–495. (b) Withersby, M. A.; Blake, A. J.; Champness, N. R.; Hubberstey, P.; Li, W. S.; Schroder, M. *Angew. Chem., Int. Ed.* **1997**, *36*, 2327–2329.

Scheme 1



three-dimensional (3D) porous MOFs, the metal–organic nanotubes possess nearly 1D structures, a uniform single wall, and unique material properties, which may result in different adsorption properties. It has been reported that the 0D squares are connected from the vertexes by a bridging organic ligand to generate a 1D interpenetrating metal–organic nanotube.¹³ Very recently, a novel noninterpenetrating metal–organic nanotube (denoted as **MONT-1**), which can reversibly absorb $(\text{H}_2\text{O})_{12}$ clusters, has also been documented by our group (Scheme 1).¹⁴ However, in reality, the connection of the 1D helix to generate novel metal–organic nanotubes has not been explored prior to the present report. Herein, reported are two novel noninterpenetrating polymorphic metal–organic nanotubes, $\text{Zn}(\text{ATIBDC})(\text{bpy})\cdot 3\text{H}_2\text{O}$ (**MONT-1** and **MONT-2**, where $\text{H}_2\text{ATIBDC} = 5\text{-amino-2,4,6-triiodoisophthalic acid}$ and $\text{bpy} = 4,4\text{-bipyridine}$), which are generated by ATIBDC ligands connecting a 0D square or a 1D helix.¹⁵

MONT-2 can be isolated from the mother liquor of **MONT-1**. When the mother-liquor-containing **MONT-1** was sealed and left at room temperature for 4 weeks, light-yellow needlelike crystals of **MONT-2** were formed. The two phases can be manually separated for further analysis.

MONT-1 and **MONT-2** have identical framework formulas and can be classified as polymorphic structures.¹⁶ Single-crystal X-ray diffraction studies reveal that **MONT-2** crystallizes in tetragonal space group $I4_1/a$. Similar to **MONT-1**, the asymmetric unit of **MONT-2** consists of one Zn ion, one ATIBDC, one bpy, and three uncoordinated water molecules. The coordination environment of the central Zn ion remained unchanged with **MONT-1**, although the average Zn–O and Zn–N distances changed a little (2.107 and 2.081 Å for Zn–O and Zn–N, respectively). The most significant structural change is that the squares (Figure 1a) in **MONT-1** are replaced with a 1D left- or right-handed 4_1 helical chain in **MONT-2** (Figure 1b), similar to that found in $\{[\text{Ni}(4,4\text{'-dipy})(\text{ArCOO})_2(\text{MeOH})_2]_n\}$.^{12a} The average dihedral angle between the carboxylate groups and the central benzene ring is 91.65° , which is slightly larger than that in **MONT-1**. The shape of the square channel remains unchanged (Figure 1c,d). The dimensions of the channel are reduced from 11.81×11.81 Å in **MONT-1** to 10.9×10.9 Å in **MONT-2**. Similar to **MONT-1**, the 1D nanotubular coordination polymers in **MONT-2** stack each other without interpenetration through the weak $\text{N}\cdots\pi$ (3.325 Å) and $\text{I}\cdots\text{O}$ (3.261 Å) interactions to generate a 3D porous supramolecular architecture (Supporting Information). The left- and right-handed 4_1 helical chains are alternatives to the 3D packing structure; thus, the whole structure is achiral.

Another significant change is the arrangement of the uncoordinated water molecules¹⁷ due to the different space groups as well as the different environments of the channels. In **MONT-1**, all of the uncoordinated water molecules (O01, O02, and O03) locate in the nanotube and form a $(\text{H}_2\text{O})_{12}$ cluster (Figure 2a) through hydrogen-bonding interaction. The cluster was trapped in the $\text{Zn}_8(\text{bpy})_8(\text{ATIBDC})_4$ box with a separation from one another of 9.581 Å (Figure 2d), corresponding to the unit cell length. However, in **MONT-2**, there is no significant hydrogen-bonding interaction among the uncoordinated water molecules.¹⁵ 0.25 uncoordinated water molecule (O01) resides among the 1D nanotubes by forming hydrogen bonds (2.799 Å) with the $-\text{NH}_2$ group of the ATIBDC ligand to connect four nanotubes (Supporting Information). 2.75 uncoordinated water molecules (O02, O03, and O04) locate in the nanotube. Every uncoordinated water molecule in the channel (O02, O03, and O04) is packing along the c axis to generate a 1D 4_1 helical chain (Figure 2b,c) with a separation of the water molecules of 3.705, 5.194, and 8.153 Å for O02, O03, and O04, respectively. In particular, there is strong hydrogen-bonding interaction (2.761 Å) between O04 and the uncoordinated carboxyl O atom of ATIBDC in an adjacent nanotube. All of the 1D 4_1 helical arrangements of the water molecules in the channel possess the same chirality as the 1D Zn–bpy helical chain.

(13) Wang, X. L.; Qin, C.; Wang, E. B.; Li, Y. G.; Su, Z. M.; Xu, L.; Carlucci, L. *Angew. Chem., Int. Ed.* **2005**, *44*, 5824–5827.

(14) Dai, F. N.; He, H. Y.; Sun, D. F. *J. Am. Chem. Soc.* **2008**, *130*, 14064–14065.

(15) Synthesis of **MONT-1** and **MONT-2**: $\text{Zn}(\text{NO}_3)_2\cdot 6\text{H}_2\text{O}$ (10 mg, 0.03 mmol), H_2ATIBDC (10 mg, 0.02 mmol), and 4,4'-bipy (10 mg, 0.052 mmol) were dissolved in 8 mL of a mixed solvent of N,N -dimethylformamide, EtOH, and H_2O (v/v, 5:2:1). After the reaction mixture was stirred at room temperature for 0.5 h, the resulting mixture was filtered. Diffusion of diethyl ether into the resulting clear yellow solution in a vial for 7 days yielded a large amount of yellow prismatic crystals of **MONT-1** (yield: 45%). Then the vial containing **MONT-1** was sealed and left at room temperature for 4 weeks to generate light-yellow needlelike crystals of **MONT-2** (yield: 10%). The two polymorphic complexes were manually separated for further analysis. Elem. anal. Calcd for **MONT-1**: C, 25.97; H, 1.94; N, 5.05. Found: C, 25.65; H, 1.94; N, 5.59. Elem. anal. Calcd for **MONT-2**: C, 25.97; H, 1.94; N, 5.05. Found: C, 25.85; H, 1.90; N, 5.32.

(16) Crystallographic data for **MONT-1**: $\text{C}_{18}\text{H}_{16}\text{I}_3\text{N}_3\text{O}_7\text{Zn}$, $M = 832.41$, tetragonal, space group $P4/n$, $a = b = 24.4385(2)$ Å, $c = 9.57470(10)$ Å, $U = 5718.40(9)$ Å³, $Z = 8$, $D_{\text{calcd}} = 1.934$ g cm⁻³, $\mu = 4.134$ mm⁻¹, $F(000) = 3120$, crystal size = $0.20 \times 0.10 \times 0.05$ mm³; 22 623 reflections were measured with 6649 unique reflections ($R_{\text{int}} = 0.0372$), of which 5599 [$I > 2\sigma(I)$] were used for the structure solution. Final $R1$ ($wR2$) = 0.0671 (0.1921), 289 parameters. Crystallographic data for **MONT-2**: $\text{C}_{18}\text{H}_{16}\text{I}_3\text{N}_3\text{O}_7\text{Zn}$, $M = 832.41$, tetragonal, space group $I4_1/a$, $a = b = 34.3706(11)$ Å, $c = 9.5456(6)$ Å, $U = 11276.6(9)$ Å³, $Z = 16$, $D_{\text{calcd}} = 1.961$ g cm⁻³, $\mu = 4.193$ mm⁻¹, $F(000) = 6240$, crystal size = $0.20 \times 0.10 \times 0.05$ mm³; 32 300 reflections were measured with 6501 unique reflections ($R_{\text{int}} = 0.0538$), of which 5937 [$I > 2\sigma(I)$] were used for the structure solution. Final $R1$ ($wR2$) = 0.0582 (0.1744), 291 parameters.

(17) In the crystal structure, some water molecules are disordered. However, the existence of three water molecules is further determined by TGA and elemental analysis.

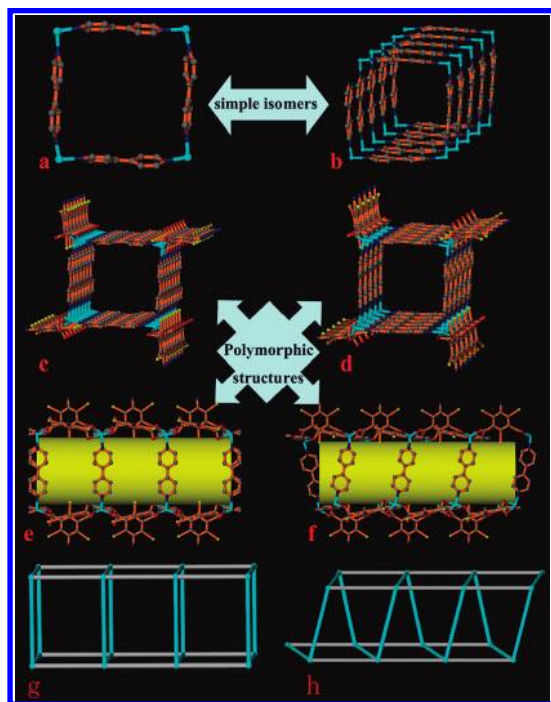


Figure 1. (a and b) Structural supramolecular isomers of a 0D square and a 1D helix in **MONT-1** and **MONT-2**, respectively. 1D nanotubes along the *c* axis: (c) **MONT-1**; (d) **MONT-2**. (e and f) Nanotubular structures of **MONT-1** and **MONT-2** showing the tube interior (yellow column). (g and h) Schematic representations of the two polymorphic structures.

Thermogravimetric analysis (TGA) measurement reveals that both **MONT-1** and **MONT-2** can be stable up to 300 °C. It is especially interesting to note that both nanotubular materials can remain crystalline at high temperature and the uncoordinated water molecules can be reversibly absorbed into the nanotubes. For **MONT-1**, the (H₂O)₁₂ cluster can be reversibly trapped in the Zn₈(bpy)₈(ATIBDC)₄ box after the crystals were heated to 180, 200, 240, and 280 °C for 0.5 h and cooled back down to room temperature in air. However, for **MONT-2**, only part of the uncoordinated water molecules can be reversibly absorbed into the channel. Single-crystal X-ray diffraction on the crystal of **MONT-2** that was heated to 160 °C for 0.5 h in air reveals that only two uncoordinated water molecules (O03 and O04) were reabsorbed into the nanotube. The separation of the water molecules in the 1D helical water chain changes to 5.882 and 8.225 Å for O03 and O04, respectively. When the crystals were heated to 200 °C, single-crystal X-ray diffraction shows that only O04 was reabsorbed into the nanotube because of its formation of strong hydrogen bonds with the uncoordinated carboxyl O atom. These results indicate that the uncoordinated water molecules are apt to be reabsorbed inside the nanotube rather than outside the nanotube.

In conclusion, two novel polymorphic metal–organic nanotubes, derived from two structural supramolecular

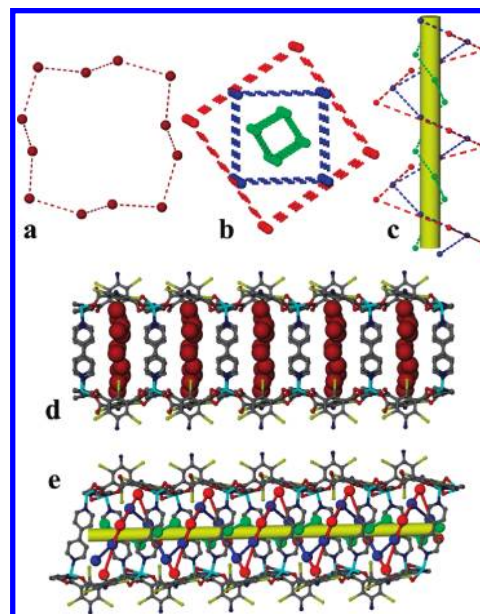


Figure 2. (a) (H₂O)₁₂ cluster in **MONT-1**. (b and c) 1D helical arrangement of the uncoordinated water molecules in **MONT-2** (green, O02; blue, O03; red, O04). (d and e) 1D nanotubes showing the arrangement of the uncoordinated water molecules in the channels for **MONT-1** and **MONT-2**, respectively.

isomers, a 0D square and a 1D helix, have been synthesized and characterized for the first time. The uncoordinated water molecules have different arrangements [a (H₂O)₁₂ cluster vs a 1D helix] in the nanotubes because of the different environments of the channels. The new nanotubular isomer can remain crystalline at high temperature and reversibly absorb uncoordinated water molecules. Although detailed studies are still needed, formation of the two polymorphic complexes may be controlled by the concentration of the reaction system, and the generation of polymorphs in this system may derive from the fact that connection of a metal ion by bpy ligands can potentially form two structural subunits, a 0D square and a 1D helix, between which there is little or no difference in formation energy. Current research provides an effective strategy to construct polymorphic structures by use of structural supramolecular isomers and may gain an in-depth understanding of polymorphism in MOFs. Further studies will focus on producing other metal–organic nanotubes by using a wide range of bridging organic ligands.

Acknowledgment. We are grateful for the financial support of the NSF of China (Grant 20701025), the NSF of Shandong Province (Grant Y2008B01), and Shandong University.

Supporting Information Available: Experimental procedures, structural figures, TGA, and crystallographic data in CIF format. This material is available free of charge via the Internet at <http://pubs.acs.org>.